JCB Article

Bld10p, a novel protein essential for basal body assembly in *Chlamydomonas*: localization to the cartwheel, the first ninefold symmetrical structure appearing during assembly

Kumi Matsuura,[1] Paul A. Lefebvre,[2,3] Ritsu Kamiya,[1,4] and Masafumi Hirono[1]

[1]Department of Biological Sciences, University of Tokyo, Tokyo 113-0033, Japan
[2]Department of Genetics, Cell Biology and Development and [3]Department of Plant Biology, University of Minnesota, St. Paul, MN 55108
[4]Core Research for Evolutional Science and Technology (CREST), Japan Science and Technology Corporation (JST), Nagoya 450-0003, Japan

How centrioles and basal bodies assemble is a long-standing puzzle in cell biology. To address this problem, we analyzed a novel basal body-defective *Chlamydomonas reinhardtii* mutant isolated from a collection of flagella-less mutants. This mutant, *bld10*, displayed disorganized mitotic spindles and cytoplasmic microtubules, resulting in abnormal cell division and slow growth. Electron microscopic observation suggested that *bld10* cells totally lack basal bodies. The product of the *BLD10* gene (Bld10p) was found to be a novel coiled-coil protein of 170 kD. Immunoelectron microscopy localizes Bld10p to the cartwheel, a structure with ninefold rotational symmetry positioned near the proximal end of the basal bodies. Because the cartwheel forms the base from which the triplet microtubules elongate, we suggest that Bld10p plays an essential role in an early stage of basal body assembly. A viable mutant having such a severe basal body defect emphasizes the usefulness of *Chlamydomonas* in studying the mechanism of basal body/centriole assembly by using a variety of mutants.

Introduction

The centriole, present at the core of the centrosome in animal cells, and basal bodies, structures that nucleate the assembly of cilia and flagella, are homologous organelles with nine triplet microtubules arranged in rotational symmetry. In *Chlamydomonas reinhardtii*, the basal body functions as the centriole during mitosis, and it subtends the flagellum in interphase cells. These organelles have long attracted attention from many researchers because of their elaborate structure and complex mechanism of assembly, which involves semi-conservative duplication once per cell cycle (for review see Dutcher, 2003).

The process of centriole/basal body assembly has been extensively studied by EM (Stubblefield and Brinkley, 1967; Dippel, 1968; Allen, 1969; Cavalier-Smith, 1974). The assembly process consists of several distinct steps: (a) an amorphous ring-like structure appears by the side of the mother organelle (Dippel, 1968); (b) a cartwheel structure consisting of a central hub and nine spokes is formed on the ring-like structure (Cavalier-Smith, 1974); (c) the A-tubule of the triplet microtubule is placed at each tip of the cartwheel spoke; (d) the B- and C-tubules are then added to the preexisting A-tubule; and (e) a cylinder consisting of nine triplet microtubules elongates to the mature length (Allen, 1969; Cavalier-Smith, 1974). Because the cartwheel structure displays ninefold symmetry, as does the mature basal body, this structure has been suggested to be the organizing center for the assembly of the microtubule wall (Anderson and Brenner, 1971; Gavin, 1984). However, no direct evidence has been reported for the importance of cartwheels in centriole/basal body assembly.

Address correspondence to Masafumi Hirono, Dept. of Biological Sciences, University of Tokyo, Bunkyo-ku, Tokyo 113-0033, Japan. Tel.: 81-3-5841-4429. Fax: 81-3-5802-2734. email: hirono@biol.s.u-tokyo.ac.jp

K. Matsuura's present address is Molecular Membrane Biology Laboratory, RIKEN, 2-1 Hirosawa, Wako, Saitama 351-0198, Japan.

Key words: centriole; centrosome; mitotic spindle apparatus; flagella; coiled-coil

Abbreviations used in this paper: BAC, bacterial artificial chromosome; NFAp, nucleoflagellar apparatus.

Little is known about the molecular mechanism controlling the assembly of centrioles/basal bodies. Molecular dissection of the assembly process is complicated by the fact that isolation and biochemical analysis of basal bodies is very difficult. Such a complex process, not amenable to biochemical analysis, is best studied by the analysis of mutants affecting the process. Recently, genetic approaches using unicellular organisms, such as *Chlamydomonas* and *Paramecium*, have identified several proteins crucial for the assembly of basal bodies and their associated structures (Taillon et al., 1992; Ruiz et al., 1999, 2000; Silflow et al., 2001). In *Chlamydomonas,* two basal body-defective mutants, *bld2* and *uni3,* have led to the discovery of ε-tubulin and δ-tubulin, respectively, and elucidation of their roles in basal body assembly (Dutcher and Trabuco, 1998; Dutcher et al., 2002). The *bld2* mutation causes cells to assemble severely truncated basal bodies composed of singlet microtubules. The *uni3* mutation causes cells to assemble incomplete basal bodies comprised of doublet, not triplet, microtubules. Therefore, the minor tubulin species ε- and δ-tubulin are thought to function in adding B- and C-tubules of basal bodies, respectively. These works demonstrate the usefulness of *Chlamydomonas* mutants for the molecular dissection of basal body assembly (Dutcher, 2003).

Here, we produced a collection of flagella-less mutants by insertional mutagenesis and isolated a new mutant, *bld10*. This mutant is defective in mitosis, frequently shows aberrant mitotic spindles and disorganized microtubule organization within the cell, and grows significantly slower than wild type. Surprisingly, EM failed to detect any basal body-like structures in this mutant. We show that the gene responsible for the *bld10* mutation codes for a novel coiled-coil protein that localizes to the cartwheel, which is a structure that is present at the proximal end of the basal body and may function as a scaffold essential for basal body assembly.

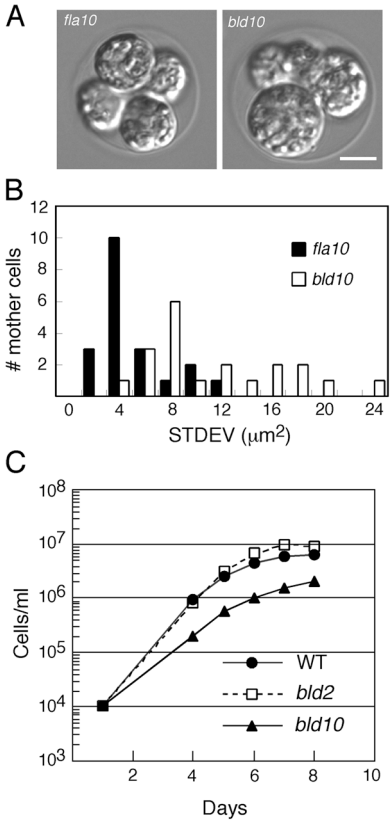

Figure 1. **Defects of *bld10* in cell division.** (A) DIC images of *bld10* and *fla10* cells. The mutant *fla10* lacks flagella but divides normally into four equal-sized daughter cells. In contrast, the daughter cells of *bld10* differ in size from cell to cell. Bar, 5 μm. (B) Histograms showing the size variability among the four daughter cells soon after division in *bld10* and *fla10*. Ordinate: the number of mother cells counted. Abscissa: the SD of the size of the four daughter cells. The size of each cell was assessed by measuring the area of two-dimensionally projected microscope images. (C) Growth rates. *bld10* grows more slowly than wild type (WT). In contrast, the growth rate of *bld2-1* is indistinguishable from that of wild type.

Results

Mitotic defects in *bld10*

To isolate mutants defective in basal body assembly, we screened ~10,000 mutants generated by insertional mutagenesis and analyzed those mutants that did not assemble flagella (Tam and Lefebvre, 1993; Matsuura et al., 2002). Of 74 flagella-less mutants isolated, one mutant (2H4) showed abnormal cell division (see next paragraph). Because the basal body-deficient mutant *bld2* displays abnormal cell division (Ehler et al., 1995), we anticipated that mutant 2H4 might also have some defects in the basal body. The mutant 2H4 was distinct from *bld2* as shown by the fact that mating between the two mutants gave rise to daughter cells with a wild-type phenotype (unpublished data). We named this mutant *bld10*.

We compared the generation time of *bld10, bld2*, and wild type. As shown in Fig. 1 C, *bld10* grew much more slowly than wild type. The growth rate of *bld10* was about one fifth that of wild type. In contrast, *bld2* grew at almost the same rate as wild type, in agreement with the description by Goodenough and St. Clair (1975). Microscopic observation indicated that the size of *bld10* cells was highly variable (Fig. 1 A). The variability among the sister cells within a common mother cell wall was quantified by measuring the area of projected cell images (Fig. 1 B). The root-mean-square difference in the area of sister cells in *bld10* was 10.2 μm^2, whereas it was 4.0 μm^2 in a null allele of *fla10*, an aflagellate strain that undergoes normal cell division (Matsuura et al., 2002). The variable cell size in *bld10* indicates that this mutant divides unequally possibly due to defects in cell division, similar to the differences in the sizes of *bld2* sister cells within a common mother cell wall (Ehler et al., 1995).

We next observed mitotic spindles in wild-type and *bld10* cells by indirect immunofluorescence microscopy using anti–α-tubulin antibody to determine whether *bld10* cells have defects in mitotic spindles. As shown in Fig. 2 A, *bld10* cells frequently formed aberrant spindles. Nuclear segregation during cell division in *bld10,* as in *bld2,* often fails (Table I), probably as the result of abnormal mitosis.

Cytoskeletal disorganization in *bld10*

Basal bodies/centrioles are known to serve as microtubule-organizing centers in interphase cells. In wild-type *Chlamydomonas*, basal bodies are associated with four microtu-

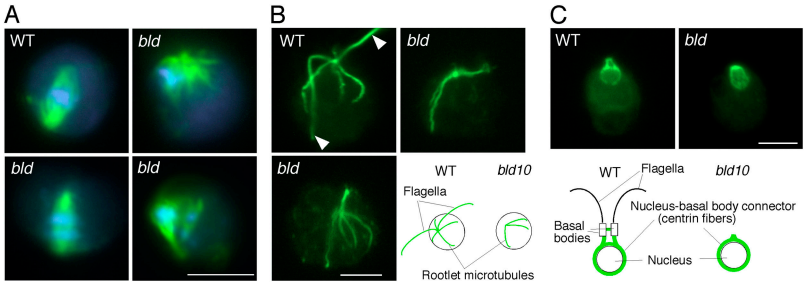

Figure 2. **Disorganized cytoskeletons in *bld10*.** (A) Spindle microtubules were visualized by indirect immunofluorescence microscopy using anti–α-tubulin antibody (green). DAPI staining is shown in blue. (B) Rootlet microtubules visualized using antiacetylated α-tubulin antibody. The arrowheads indicate flagella. The number and position of rootlets are aberrant in *bld10*. Similar results were obtained with *bld2* (Ehler et al., 1995). Diagrams represent typical staining patterns in wild-type and *bld10* cells. Structures stained with the antibody are shown in green. (C) Centrin-containing fibers visualized using anticentrin antibody. In wild-type cells, the so-called diamond ring pattern can be seen. In *bld10* cells, no such a distinct pattern was found. Diagrams represent typical staining patterns in wild-type and *bld10* cells. Centrin-containing fibers are shown in green. (WT) wild type, (*bld*) *bld10*. Bars, 5 μm.

bule bundles called the rootlet microtubules, which play an important role in determining the position of the cleavage furrow (Ehler et al., 1995). To examine the organization of the rootlets in *bld10*, cells were stained with an antibody to acetylated α-tubulin (Fig. 2 B). Wild-type cells show a cruciform pattern of rootlet microtubules radiating from the vicinity of the basal bodies. In *bld10* cells, however, the number of the rootlet microtubule bundles was frequently less than or greater than four. The arrangement of those bundles was also aberrant.

Another intracellular structure associated with the basal bodies is the system of centrin-containing fibers connecting the basal bodies to the nucleus (Huang et al., 1988). We examined these fibers using immunofluorescence microscopy with an anticentrin antibody in wild-type cells and in *bld10* mutant cells (Fig. 2 C). In *bld10* cells we were unable to visualize centrin-containing projections comparable to those seen in wild-type cells. *bld2* cells have similar, severe defects in the assembly of centrin-containing fibers (Ehler et al., 1995).

Electron microscopic observation of basal bodies of *bld10*

We were unable to observe any basal body-like structures in *bld10* cells despite extensive examination of more than 1,000 thin sections. Instead, we very rarely observed structures that resembled flagellar membranes protruding from the cell body without an accompanying basal body nearby (Fig. 3, B and C). Beneath the protrusion, rootlet microtubules and the distal striated fibers, which in the wild-type cells would connect the two basal bodies, were occasionally found, but they were aberrantly positioned. These observations suggest that *bld10* lacks morphologically identifiable basal bodies.

Cloning and characterization of the *BLD10* gene

The *BLD10* gene was cloned using the plasmid tag inserted into the genome of the *bld10* mutant (Tam and Lefebvre, 1993). Southern blots using genomic DNA showed that *bld10* has a single plasmid insertion. Backcrosses of *bld10* to wild-type cells showed Mendelian segregation of the aflagellate phenotype consistent with a mutation caused by the insertion of the nitrate reductase gene into a single genetic locus (unpublished data). By screening a bacterial artificial chromosome (BAC) library using the genomic fragment flanking the inserted plasmid as a probe, we isolated seven clones with inserts ranging from 21 to ~100 kb (Fig. 4). All clones were found to rescue the *bld10* phenotype upon introduction of BAC DNA into mutant cells by electroporation. By repeated transformation with those clones after digestion with appropriate restriction enzymes, we found that the region necessary for rescue can be reduced to 13 kb. Analyses of the sequence using the GeneMark and GreenGenie gene prediction programs (Lukashin and Borodovsky, 1998; Kulp et al., 1996) consistently predicted that the fragment contains a single gene consisting of 27 exons extending over 12 kb. The exon–intron boundaries of the predicted gene were confirmed by sequencing DNA fragments produced by RT-PCR using primers designed from the predicted exon regions. Using PCR-based polymorphisms (Kathir et al., 2003) the cloned *BLD10* gene was mapped at the end of Linkage Group X, 6 cM centromere-distal to *PF24* (unpublished data). No uncharacterized flagellar-assembly mutations have been mapped to this region of the genome, so *BLD10* is a novel genetic locus.

Analysis of the complete cDNA sequence showed that *BLD10* has a single ORF of 4,923 bp that encodes a predicted protein (Bld10p) of 1,640 aa with a predicted molecular mass of 174.6 kD (Fig. 5 A). Bld10p has a high probability of forming coiled coils over its entire length (Fig. 5 B), as predicted using the COILS algorithm (Lupas et al., 1991). A consensus sequence for the myosin-tail domain and two leucine zipper motifs were found in the COOH-terminal half (Fig. 5, A and C). Bld10p as a whole showed no significant homology with any known protein sequence. However, a group of uncharacterized mammalian proteins, including human KIAA0635 and mouse BC062951, are distantly related to Bld10p. Although sharing only 25% identity in a limited region of the sequence, these proteins are predicted to form a coiled-coil structure throughout their length like Bld10p.

While cloning the *BLD10* gene, we were surprised to find that genomic fragments lacking part of the NH_2-terminal re-

Table I. **Number of nuclei per cell**

Number of nuclei/cell	0	1	2	3
	%	%	%	%
wild type (*n* = 388)	0.0	99.2	0.8	0.0
bld10 (*n* = 443)	2.7	91.0	6.1	0.2
bld2-1 (*n* = 470)	2.3	87.4	9.6	0.6

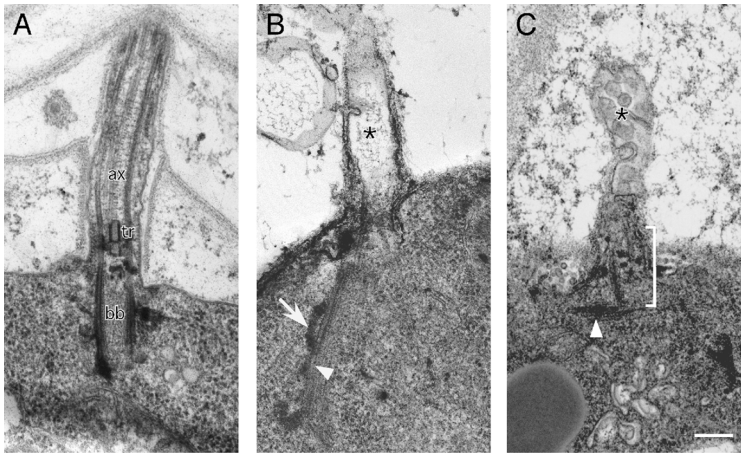

Figure 3. **Electron microscopic observation of *bld10* cells.** (A) Image of wild-type cells showing the basal body (bb), transitional region (tr), and axoneme (ax). (B and C) images from *bld10* samples. (B) A flagellar membrane-like structure protruding from the cell body (asterisk), microtubule bundles (arrowhead) reminiscent of rootlet microtubules and an aberrantly positioned striated fiber (arrow) are seen. However, no basal body was found around these structures. (C) Another example of membranous projection in *bld10* (asterisk). Short microtubule bundles (arrowhead) were also seen. Bracket shows the position where a basal body would appear if this protrusion is in fact a normal flagellum. Bar, 200 nm.

gion of the gene rescued the mutation as efficiently as the full-length gene (Fig. 4). Even when we deleted the NH_2-terminal 30% of the gene (fragment ΔN), the mutant phenotype was rescued completely, indicating that the NH_2-terminal part of Bld10p is not essential for its function.

Localization of Bld10p

The localization of Bld10p in the cell was examined using a polyclonal antibody raised against a bacterially expressed peptide (Fig. 5 A). Fig. 6 A shows the specificity of this antibody by Western blot analysis of proteins in the whole cell extracts. Proteins from wild–type cells yielded a single immunoreactive band with an apparent molecular mass of 170 kD, whereas the extract from *bld10* mutants yielded no band. A band of the same size was detected in the extract from *bld10* cells rescued with a BAC clone containing the full-length *BLD10* gene. A smaller molecular mass band (~120 kD) was detected in the cells transformed with the DNA fragment truncated at the NH_2-terminal end (ΔN). An extract from the *bld2* mutant also displayed a band of 170 kD. To determine whether Bld10p is associated with the basal body or its related structures, we analyzed the nucleoflagellar apparatuses (NFAPs), i.e., cytoskeletal complexes containing the basal bodies, axonemes, rootlet microtubules, nuclei, and other fibrous structures connected to the basal bodies (Wright et al., 1985). The antibody, while detecting no band in axonemal samples, detected a band in NFAPs stronger than in the extract from whole cells (Fig. 6 B), suggesting that the protein resides in the basal body region of the NFAPs and not in the axoneme.

Indirect immunofluorescence microscopy confirmed the association of Bld10p with the basal body. When the NFAPs from flagellated interphase cells were stained, three or four dots were visible at the position of the basal bodies (Fig. 6 C). The presence of more than two dots suggests that this protein is localized also to the probasal bodies, the precursor of the basal bodies, that are present throughout the G1 phase of the cell cycle (Gaffal, 1988). In mitotic cells, in which flagella are resorbed and the two mother–daughter basal body pairs are located near the spindle poles, Bld10p was found localized at the spindle poles (Fig. 6 C). Thus, Bld10p appeared to be localized to the basal body/centrioles throughout the cell cycle. The mutant *bld2* expresses Bld10p at levels comparable to wild-type cells (Fig. 6 A). Bld10p was correctly localized at the position of the basal bodies in *bld2* cells, although only one or two dots of Bld10p fluorescence were usually visible (Fig. 6 D). This result suggests that Bld10p is incorporated during assembly of basal bodies at a step before the *BLD2* gene product, ε-tubulin.

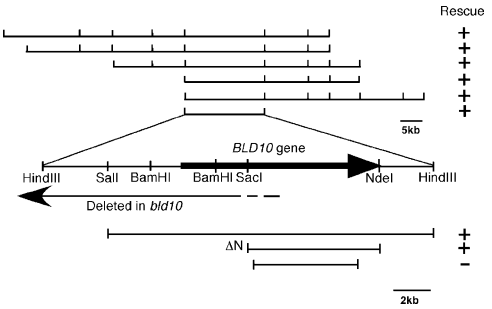

Figure 4. **Genomic clones containing the *BLD10* gene.** (Top) Six BAC genomic clones containing the region flanking the plasmid insertion. All of these clones were found to rescue the *bld10* mutation upon introduction into the cell by transformation. (Middle) Restriction map of the *BLD10* gene. The bold arrow indicates the region of the *BLD10* gene. (Bottom) DNA fragments used for the rescue experiment. Note that a construct lacking ~30% of the NH_2 terminus region (ΔN) was sufficient to rescue *bld10*.

Immuno-EM

To further define the cellular localization of Bld10p, we next performed immuno-EM on the isolated NFAPs. Gold particles conjugated to the secondary antibody were found at the proximal end of the basal bodies in longitudinal sections (Fig. 7 A). In cross sections, particles were found on radial thin filaments in the lumen of the basal body (Fig. 7 B). Bld10p was localized to the structure called the cartwheel, a subcentriolar structure present near the proximal end of the organelle. It is composed of the central tubule and a group of nine filaments radiating from the tubule to each triplet microtubule. Several sets of the nine filaments are usually present in a single centriole/basal body (Gibbons and Grimstone, 1960). The cartwheel makes up a hub and spokes with ninefold symmetry. During the assembly of the centriole/basal body, the cartwheel appears in the earliest stage, when its basement structure is assem-

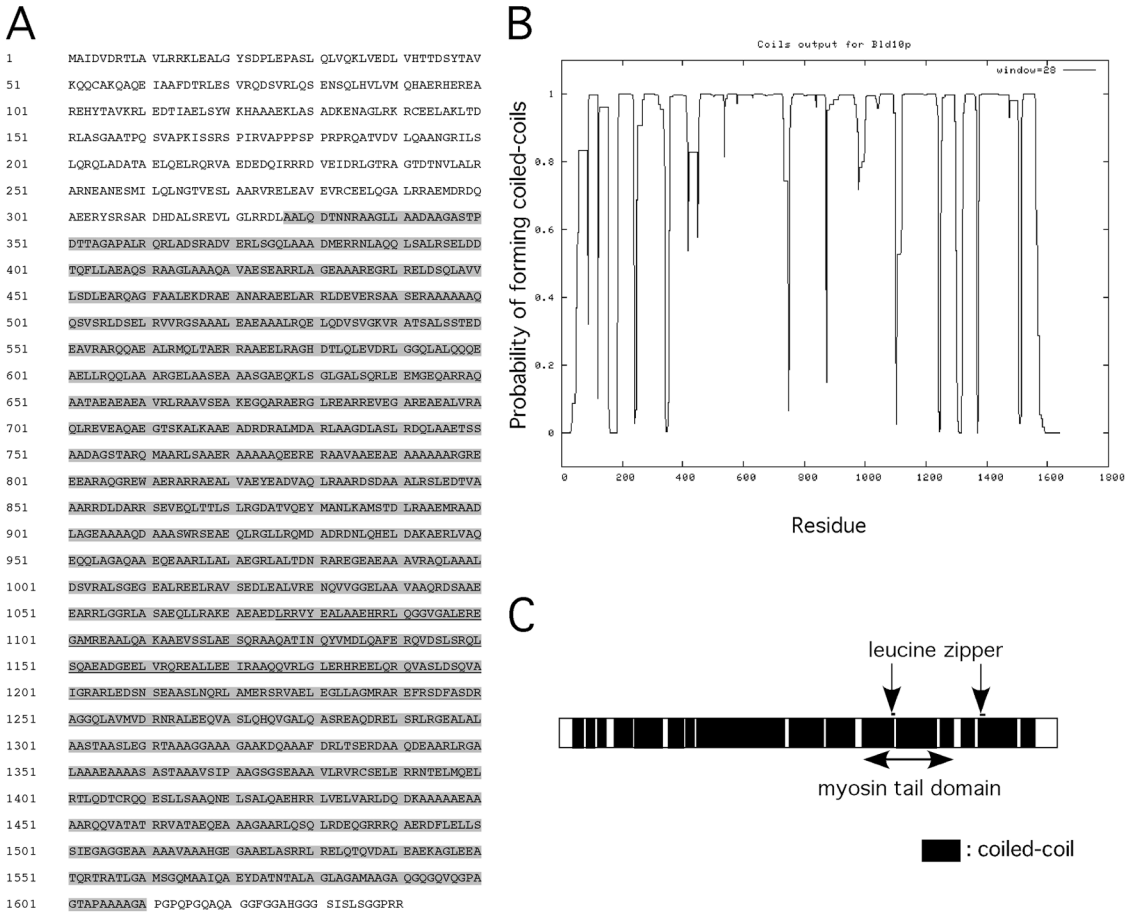

Figure 5. **Sequence and predicted secondary structure of Bld10p.** (A) Amino acid sequence of Bld10p. Shaded regions indicate an alanine-rich region. Underlined sequence was used for antibody production. (B) Prediction of the coiled-coil region using the COILS program. (C) Schematic diagram of Bld10p. Arrows indicate positions of the leucine zipper motifs, which may participate in protein–protein interaction. A motif of the myosin tail domain is indicated with a bidirectional arrow. These sequence data are available from GenBank/EMBL/DDBJ accession no. AB116368.

bled (Anderson and Brenner, 1971). In agreement with this observation, the Bld10p signal was also observed in the probasal body, an immature basal body developing beside the mother basal body (Fig. 7 C).

Discussion

In this paper we show that the *BLD10* gene of *Chlamydomonas* is required for basal body assembly. The *BLD10* gene product localizes to the cartwheel, a ninefold symmetrical structure that appears in the early stage of the centriole/basal body assembly.

Extensive electron microscopic observations failed to detect any basal body-like structures in the *bld10* cells (Fig. 3). We conclude that this mutant totally lacks basal bodies, although we cannot rule out the possibility that some disorganized basal body-related structure was present and not detected in our electron micrographic analysis. Whether or not some small basal body remnant is present in mutant cells, however, *bld10* cells clearly have severe defects in basal body assembly. Some of the defects in *bld10* have also been observed in *bld2*, a mutant that has severely disrupted basal bodies, formed at most of short, singlet microtubules (Goodenough and St. Clair, 1975; Ehler et al., 1995). Both mutants frequently show abnormality in the position of the cleavage furrow, resulting in the production of daughter cells of unequal sizes and containing an abnormal number of nuclei (Fig. 1 and Table I). Both display abnormality in the cytoskeletons associated with the basal body, e.g., rootlet microtubules and nucleus-basal body connectors (Fig. 2 C), and abnormal spindles in mitotic cells (Fig. 2 A). These defects are closely related to each other because the rootlet microtubules function in determining the position of the spindle and cleavage furrow just like astral microtubules in animal cells (Ehler et al., 1995). The deficiencies shared by *bld10* and *bld2* indicate that both mutants are commonly deficient in some basal body-related structures required for the precise arrangement of cytoskeletal structures.

However, *bld10* also displays some defects that have not been observed in *bld2*. Most strikingly, the apparent generation time of *bld10* was much longer than that of *bld2,* which grows almost as fast as wild type (Fig. 1). In addition, *bld10* often forms abnormal spindles with microtubules not tied to the spindle poles, whereas *bld2* forms normal, albeit aberrantly positioned, spindles (Fig. 2 A; Ehler et al., 1995). The slow growth of *bld10* might be due to the operation of a

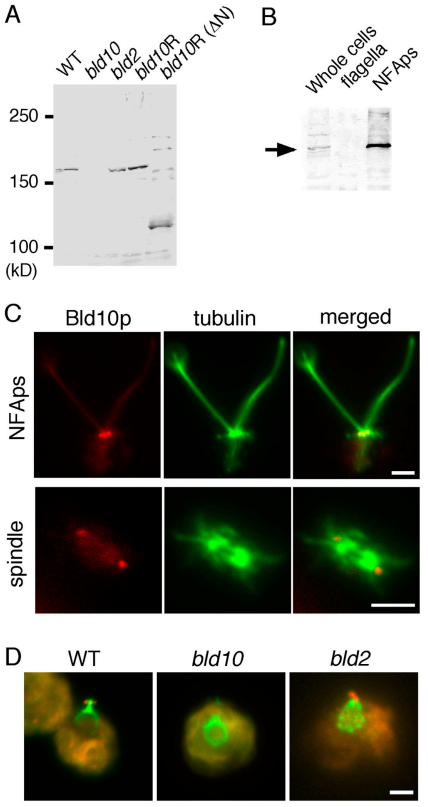

Figure 6. **Bld10p localizes to basal bodies/centrioles.** (A) Immunoblot with anti-Bld10p pAb raised against a COOH-terminal region of Bld10p. Whole cell extracts from wild-type (WT), *bld10*, *bld2*, and *bld10* cells rescued with a BAC clone (*bld10*R), and *bld10* cells rescued with a truncated fragment (*bld10*R [ΔN]). A 170-kD band was detected in extracts from cells containing the full-length *BLD10* gene, whereas a 120-kD band was detected in the *bld10*R(ΔN) extract. (B) Bld10p is enriched in NFAps. Immunoblot analysis of whole cell extract (10 μg/lane), isolated flagella (10 μg/lane), and NFAps (2 μg/lane). Bld10p signal (arrow) is absent in flagella but strong in NFAp samples. (C) Bld10p localized to basal bodies/centrioles throughout the cell cycle. NFAp (top) or mitotic spindle (bottom) were double stained with anti-Bld10p (red) and anti–α-tubulin antibody (green). Bld10p signal was detected at the base of the flagella and at the spindle poles. (D) Bld10p localized to the basal body remnants of *bld2* cells. Indirect immunofluorescence microscopy in which cells were double labeled with anti-Bld10p antibody (red) and anticentrin antibody (green). The structure of centrin-containing fibers was disrupted in both *bld10* and *bld2* (Ehler et al., 1995). In the wild-type cell, three dots of Bld10p are visible at a position on the basal bodies. Unlike wild-type cells, *bld2* cells displayed no more than two dots. The orange color of the cell body is due to the chloroplast autofluorescence. Bars, 2 μm.

checkpoint mechanism that inhibits cell division until spindle microtubules are correctly connected to the kinetochores and spindles. These differences suggest that *bld10* basal body defects may be more severe than those in *bld2* mutant cells.

Immunoelectron microscopic observations showed that Bld10p localizes to a distinct structure in the centriole, called the cartwheel (Fig. 7). The cartwheel structure has been found in the procentrioles or probasal bodies in many organisms. In vertebrates, it is present in the procentriole but disappears from the mature centriole, whereas in alga and ciliated cells it is retained in the basal body throughout the cell cycle (Alvey, 1986). Previous works described the

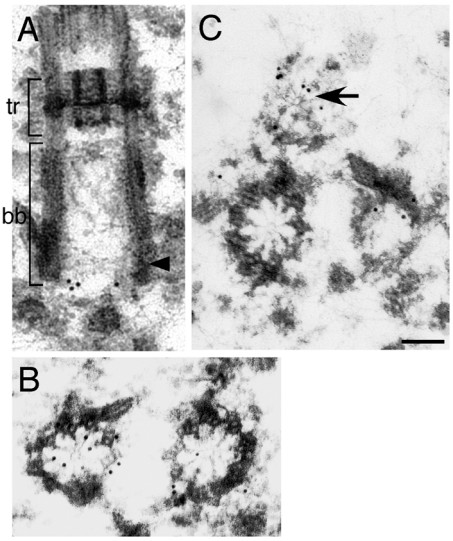

Figure 7. **Bld10p localizes to the proximal end of the basal bodies.** Immunoelectron micrographs of isolated NFAps labeled with anti-Bld10p antibody. (A) Longitudinal section of the basal body (tr, transitional region; bb, basal body). Secondary antibody conjugated with 10-nm gold is located at the proximal end of the basal body. Cartwheel fibers are faintly seen (arrowhead). (B) Cross section of a basal body pair decorated with gold particles. The presence of cartwheels indicates that this section shows the proximal part of the basal body. (C) Bld10p staining was also detected in probasal bodies (arrow). Note that probasal bodies with partially assembled cartwheel fibers also are labeled with anti-Bld10p antibody. Bar, 100 nm.

cartwheel as the first ninefold symmetrical structure that appears in the process of centriole/basal body assembly (Anderson and Brenner, 1971; Cavalier-Smith, 1974; Tamm and Tamm, 1980; Kallenbach, 1982; Fig. 8). Thus, the cartwheel has been proposed to function as a scaffold essential for centriole/basal body assembly (Anderson and Brenner, 1971). In the absence of genetic analysis, however, the functional importance of the cartwheel in the centriole/basal body assembly has not been established. The absence of

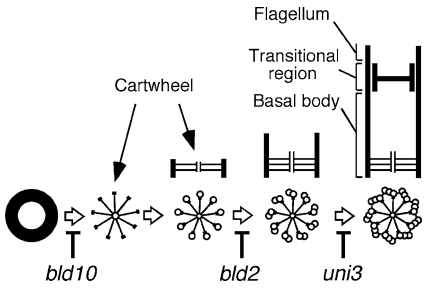

Figure 8. **Possible roles of cartwheels and Bld10p in basal body formation.** Schematic diagrams showing the pathway of basal body formation. The bottom row shows the cross-sectional view of basal bodies at the proximal end. The top row shows the longitudinal cross section. The cartwheel appears in an early stage of the assembly process. Microtubules emerge from the cartwheel filament tips and elongate distally during maturation. Bld10p may function in cartwheel assembly, possibly as a component of the cartwheel itself. The black ring in the first step is an amorphous structure appearing at the first step of basal body assembly; for clarity it is omitted in the diagrams of subsequent steps.

basal bodies in *bld10* cells and the localization of Bld10p to the cartwheel suggests that the cartwheel must play a crucial role in the assembly of the centriole/basal body (Fig. 8).

Sequence analysis indicates that Bld10p has a strong tendency to form coiled coils over its entire length, with two leucine zipper motifs and a domain homologous to the myosin tail. Hence, Bld10p is likely to be an elongated protein capable of interacting with other proteins or with itself. Bld10p might well be the major structural component of the cartwheel, which is made up of thin filaments. Rather surprisingly, we found that a Bld10p variant from which the NH_2-terminal 30% has been removed can rescue the mutation as efficiently as intact Bld10p. The structure of the basal bodies observed by thin section EM in the rescued cells was indistinguishable from that in the wild-type cells (unpublished data). These observations suggest that the NH_2-terminal 30% is not necessary for the putative protein-protein interaction that underlies the cartwheel function. If Bld10p functions through its interaction with itself, this would mean that the interaction does not involve head-to-tail association; rather, the interaction may involve lateral or staggered association between the molecules, like the myosin tails in the thick filaments of skeletal muscle. Determining whether Bld10p interacts with itself or with other proteins, and elucidation of the portions of the molecule important for function awaits future study.

The viability of *bld10* cells despite their severe basal body defect raises the question whether the organelle is essential in *Chlamydomonas*. Based on the genetic analyses of *bld2*, Preble et al. (2001) suggested that the basal body is essential. The original strain of *bld2* that has a truncated gene product (ε-tubulin) shows a severe basal body defect but it is viable. However, a null allele of *bld2* isolated in a diploid strain is lethal when diploids are sporulated to produce haploids. This result strongly suggests that the *BLD2* gene plays an essential role in assembling the basal bodies and that the complete loss of the organelle should be lethal. On the other hand, the loss of Bld10p, which appears to play an essential role at an earlier step than ε-tubulin, does not result in lethality. A possible explanation for these inconsistent results is that ε-tubulin has an essential role not only in assembling the basal body but also in another process essential for viability, for example forming cytoplasmic microtubules. The localization of ε-tubulin in material surrounding the basal bodies and in spikes protruding along rootlets, may be consistent with this possibility.

In animal cells, it is becoming evident that centrosomes are not essential for mitotic spindle formation (Rieder et al., 2001). In extracts of *Xenopus* oocytes, functional bipolar spindles were assembled in the absence of centrosomes (Heald et al., 1997). Similar results were obtained in vivo as well: when centrosomes are ablated using laser light or a microneedle, cells form acentrosomal spindles and complete mitosis (Maniotis and Schliwa, 1991; Khodjakov et al., 2000). Thus, in addition to the normal pathway for spindle assembly, cells have a centrosome-independent pathway, to which certain types of kinesin, dynactin, cytoplasmic dynein, and NuMA are known to contribute (Compton, 1998). Because the orthologues of almost all of these proteins are found in the *Chlamydomonas* genome database (http://genome.jgi-psf.org/chlre2/chlre2.home.html), it is reasonable to speculate that *Chlamydomonas* also has the redundant pathway for spindle assembly.

In summary, *bld10* lacks a protein that functions in the early stage of basal body formation. The ultrastructural defect in *bld10* cells is more extreme than the defects in any previously studied basal body mutants of *Chlamydomonas*. A simple yet important conclusion from this work is that *Chlamydomonas* mutants that have such a serious defect in the basal bodies are not lethal and can be analyzed by genetic as well as molecular biological means. We may expect that further isolation of basal body-deficient mutants will enable us to identify a variety of new basal body components and deepen our understanding of the mechanism of basal body/centriole assembly.

Materials and methods

Strains and culture conditions

For insertional mutagenesis, strain A54-e18 (*ac17 nit1* mt^+) (Smith and Lefebvre, 1996) was transformed with the plasmid pMN56 containing the *NIT1* gene (Fernandez et al., 1989). A flagella-less mutant, 2H4, generated during transformation was chosen for further analysis. Strains L5 (*nit1*, *apm1*, mt^+) and L8 (*nit1*, *apm1*, mt^-) were used in backcrosses to analyze the linkage of the *bld10* mutation in strain 2H4 to the site of plasmid insertion (Tam and Lefebvre, 1993). Strains CC-478 (*bld2*; mt^+) CC-479 (*bld2*; mt^-), and CC-503 (*cw92*; mt^+) were obtained from the *Chlamydomonas* Genetics Center. A null allele of *fla10* with an aflagellate phenotype (Matsuura et al., 2002) was used as a control for cell division experiments. For phenotypic rescue experiments, a double mutant *bld10arg7* was constructed by crossing *bld10* with an *arg7* mutant strain (lacking argininosuccinate lyase; Debuchy et al., 1989). Phenotypically rescued strains *bld10*R and *bld10*R(ΔN) were transformed with the wild-type *BLD10* gene and the gene lacking the NH_2-terminal 30% of the predicted protein, respectively. Culture media used were SGII, SGII-NO_3 (Sager and Granick, 1953; Kindle, 1990), TAP medium (Gorman and Levine, 1965), and TAP medium supplemented with 0.005% arginine. Cells were grown at 24°C on solid agar medium under constant illumination or in liquid medium on a 12 h/12 h light/dark cycle with constant aeration. Growth media was prepared as described previously (Tam and Lefebvre, 1993). Conditions for gamete production and mating were as described previously (Harris, 1989).

Transformation and phenotypic rescue experiments

For production of insertional mutants, A54-e18 cells were transformed by vortexing cells with glass beads (Kindle, 1990; Tam and Lefebvre, 1993). For rescue experiments, a *bld10arg7* double mutant strain was transformed by electroporation (Shimogawara et al., 1998) using a mixture of the plasmid pARG7.8 carrying the argininosuccinate lyase gene (Debuchy et al., 1989) and different fragments of genomic DNA. After transformation, cells were suspended in liquid TAP medium in test tubes and cultivated for 5 d. Rescue of the *bld10* phenotype was judged by observing swimming cells at the menisci of culture tubes.

Identification of the genomic region containing the *BLD10* gene

A genomic DNA fragment adjacent to the plasmid insertion site was isolated by plasmid rescue after digestion of genomic DNA using SphI (Tam and Lefebvre, 1993). Using the isolated DNA fragment as a probe, a *Chlamydomonas* BAC library (Clemson University Genomics Institute, Clemson, SC) was screened.

Determining the *BLD10* cDNA sequence

Exons in the genomic sequence were predicted using the GeneMark (Lukashin and Borodovsky, 1998) and GreenGenie programs (http://www.cse.ucsc.edu/%7Edkulp/cgi-bin/greenGenie; Kulp et al., 1996). The exon–intron boundaries of the gene were determined by RT-PCR. The first strand cDNA for RT-PCR was synthesized using RNA isolated by CsCl cushion centrifugation (Sambrook et al., 1989). The primer used for cDNA synthesis was a 20-mer oligonucleotide designed from the cloned cDNA sequence. The single strand cDNA was purified by a GLASS MAX DNA isolation spin cartridge system (GIBCO BRL). PCR was performed in the presence of 5% DMSO using the synthesized cDNA as a template,

primers designed from the putative exon sequences, and the Expand™ High Fidelity PCR System (Roche Applied Science).

Production of anti-Bld10p antibodies

For preparation of pAbs against Bld10p, a GST fusion protein carrying the sequence spanning 109 aa of the protein (Fig. 6) was expressed in *E. coli*. The cDNA sequence coding for the peptide was amplified by PCR using primers KM1 (5′-CGCGGATCCCTGCGGCGTGTTTATGAGGC-3′) and KM2 (5′-CCGGAATTCCCCTGTTACGGTCCACCATG-3′) with the cDNA isolated from the library as a template. The PCR product was digested at BamHI and EcoRI sites in the primer sequences (underlined) and subcloned into the BamHI–EcoRI sites of the pGEX2T vector (Amersham Biosciences). Expression of the fusion protein was induced by adding 0.1 mM IPTG to the *E. coli* cell culture and the whole bacterial proteins were analyzed by SDS-PAGE. After the gel was stained with Coomassie brilliant blue, the band of the fusion protein in the gel was cut out and immersed in distilled water for 30 min at RT. The gel was loaded on another SDS-polyacrylamide gel and overlaid with the SDS-PAGE sample buffer. After electrophoresis, an appropriate portion of the gel containing the protein was excised, crushed, dialyzed against PBS, and used for immunizing rabbits. The antisera were affinity purified using the fusion protein blotted on PVDF membranes (Olmsted, 1981).

Fluorescence microscopy

Indirect immunofluorescence microscopy was performed as described by Holmes and Dutcher (1989). The primary antibodies used were affinity-purified anti-Bld10p antibody, antiacetylated α-tubulin (monoclonal 6-11B-1; Sigma-Aldrich) diluted in blocking buffer to 1:50, anti–α-tubulin (monoclonal B-5-1-2; Sigma-Aldrich) to 1:100, and anticentrin antibody (a gift from J.L. Salisbury, Mayo Clinic, Rochester, MN) to 1:50. The secondary antibodies used were FITC-conjugated goat anti–mouse IgG and rhodamine-conjugated goat anti–rabbit IgG (Sigma-Aldrich). To observe the localization of DNA relative to spindle microtubules, cells were simultaneously stained with anti–α-tubulin antibody and 0.1 mg/ml DAPI. NFAps were prepared from a cell wall-less mutant, *cw92*, by the method of Silflow et al. (2001). Images were recorded using an Axioplan fluorescence microscope (Carl Zeiss MicroImaging, Inc.) with a 63×/1.4 NA plan-APOCHROMAT objective lens and a CoolSNAP CCD camera (Roper Scientific).

EM

Cells grown to log phase were collected by centrifugation and prefixed in 2% glutaraldehyde at RT for 1–2 h. After three washes in collidine buffer (Wright et al., 1983), samples were fixed after in 1% OsO_4 in collidine buffer on ice for 1 h. Samples were then dehydrated and embedded in EPON812 resin. Thin sectioned samples were stained with aqueous uranyl acetate and Reynold's lead citrate, and observed with a JEM100-CX electron microscope (JEOL). For immuno-EM, NFAps were suspended in 0.5 ml of HMT buffer (30 mM Hepes, 5 mM $MgSO_4$, 5 mM EGTA, 25 mM KCl, pH 7.0), and mixed with 0.5 ml of 6% formaldehyde/0.5% glutaraldehyde in HMT buffer. The fixation was performed on ice for 1 h. After one wash with PBS containing 50 mM NH_4Cl and two washes with PBS, the NFAps were incubated in PBS containing 1% BSA (PBS/BSA) for 2 h with gentle agitation at 4°C. The NFAps were treated with primary antibody in the PBS/BSA solution at a dilution of 1:20 at 4°C for 16 h to overnight. After three washes in PBS/BSA, the NFAps were incubated with the secondary antibody (goat anti–rabbit IgG conjugated with 10-nm gold particles) in PBS/BSA at a 1:20 dilution at RT. After one wash with PBS/BSA and three washes with PBS, the apparatuses were fixed after in 2.5% glutaraldehyde in 0.1 M phosphate buffer, pH 7.4, at RT for 1 h, and then in 1% glutaraldehyde in 0.1 M phosphate buffer, pH 7.4, at 4°C overnight. The samples were fixed after in 1% OsO_4 in 0.1 M phosphate buffer, pH 7.4, for 1 h on ice. The pellets were block-stained with 1% uranyl acetate for 1 h on ice, dehydrated, and embedded in EPON812 resin. As a negative control, primary antibody was omitted.

We would like to thank Madoka Hiraki for the help in determining DNA sequences, Takako Minoura-Kato and Ken-ichi Wakabayashi for antibody preparation, and Dr. J.L. Salisbury for anticentrin antibody. We also thank Dr. Carolyn Silflow for insightful comments on the manuscript.

This work was supported by Grants-in-Aid for Scientific Research from the Ministry of Education, Culture, Science and Technology of Japan (14658228 to M. Hirono and 14658221 to R. Kamiya), a grant from the U.S. National Institutes of Health (GM34437 to P. Lefebvre), and a grant from The Sumitomo Foundation to M. Hirono.

Submitted: 4 February 2004
Accepted: 3 May 2004

References

Allen, R.D. 1969. The morphogenesis of basal bodies and accessory structures of the cortex of the ciliated protozoan *Tetrahymena pyriformis*. *J. Cell Biol.* 40: 716–733.

Alvey, P.L. 1986. Do adult centrioles contain cartwheels and lie at right angles to each other? *Cell Biol. Int. Rep.* 10:589–598.

Anderson, R.G.W., and R.M. Brenner. 1971. The formation of basal bodies (centrioles) in the rhesus monkey oviduct. *J. Cell Biol.* 50:10–34.

Cavalier-Smith, T. 1974. Basal body and flagellar development during the vegetative cell cycle and the sexual cycle of *Chlamydomonas reinhardtii*. *J. Cell Sci.* 16:529–556.

Compton, D.A. 1998. Focusing on spindle poles. *J. Cell Sci.* 111:1477–1481.

Debuchy, R., S. Purton, and J.-D. Rochaix. 1989. The argininosuccinate lyase gene of *Chlamydomonas reinhardtii*: an important tool for nuclear transformation and for correlating the genetic and molecular maps of the *ARG7* locus. *EMBO J.* 8:2803–2809.

Dippel, R.V. 1968. The development of basal bodies in *Paramecium*. *Proc. Natl. Acad. Sci. USA.* 61:461–468.

Dutcher, S.K. 2003. Elucidation of basal body and centriole functions in *Chlamydomonas reinhardtii*. *Traffic.* 4:443–451.

Dutcher, S.K., and E.C. Trabuco. 1998. The *UNI3* gene is required for assembly of basal bodies of *Chlamydomonas* and encodes δ-tubulin, a new member of the tubulin superfamily. *Mol. Biol. Cell.* 9:1293–1308.

Dutcher, S.K., N.S. Morrissette, A.M. Preble, C. Rackley, and J. Stanga. 2002. ε-tubulin is an essential component of the centriole. *Mol. Biol. Cell.* 13: 3859–3869.

Ehler, L.L., J.A. Holmes, and S.K. Dutcher. 1995. Loss of spatial control of the mitotic spindle apparatus in a *Chlamydomonas reinhardtii* mutant strain lacking basal bodies. *Genetics.* 141:945–960.

Fernandez, E., R. Schnell, L.P. Ranum, S.C. Hussey, C.D. Silflow, and P.A. Lefebvre. 1989. Isolation and characterization of the nitrate reductase structural gene of *Chlamydomonas reinhardtii*. *Proc. Natl. Acad. Sci. USA.* 86:6449–6453.

Gaffal, K.P. 1988. The basal body-root complex of *Chlamydomonas reinhardtii* during mitosis. *Protoplasma.* 143:118–129.

Gavin, R.H. 1984. In vitro reassembly of basal body components. *J. Cell Sci.* 66: 147–154.

Gibbons, I.R., and A.V. Grimstone. 1960. On flagellar structure in certain flagellates. *J. Biophys. Biochem. Cytol.* 7:697–716.

Goodenough, U.W., and H.S. St. Clair. 1975. *BALD-2*: a mutation affecting the formation of doublet and triplet sets of microtubules in *Chlamydomonas reinhardtii*. *J. Cell Biol.* 66:480–491.

Gorman, D.S., and R.P. Levine. 1965. Cytochrome f and plastocyanin: their sequence in the photosynthetic electron transport chain of *Chlamydomonas reinhardtii*. *Proc. Natl. Acad. Sci. USA.* 54:1665–1669.

Harris, E.H. 1989. The *Chlamydomonas* Sourcebook. Academic Press, San Diego, CA. 780 pp.

Heald, R., R. Tournebize, A. Habermann, E. Karsenti, and A. Hyman. 1997. Spindle assembly in *Xenopus* egg extracts: respective roles of centrosomes and microtubule self-organization. *J. Cell Biol.* 138:615–628.

Huang, B., D.M. Watterson, V.D. Lee, and M.J. Schibler. 1988. Purification and characterization of a basal body-associated Ca^{2+}-binding protein. *J. Cell Biol.* 107:121–131.

Holmes, J.A., and S.K. Dutcher. 1989. Cellular asymmetry in *Chlamydomonas reinhardtii*. *J. Cell Sci.* 94:273–285.

Kallenbach, R.J. 1982. Origin and maturation of centrioles in association with the nuclear envelope in hypertonic-stressed sea urchin eggs. *Eur. J. Cell Biol.* 28: 68–76.

Kathir, P., M. LaVoie, W.J. Brazelton, N.A. Haas, P.A. Lefebvre, and C.D. Silflow. 2003. Molecular map of the *Chlamydomonas reinhardtii* nuclear genome. *Eukaryot. Cell.* 2:362–379.

Kindle, K.L. 1990. High-frequency nuclear transformation of *Chlamydomonas reinhardtii*. *Proc. Natl. Acad. Sci. USA.* 87:1228–1232.

Khodjakov, A., R.W. Cole, B.R. Oakley, and C.L. Rieder. 2000. Centrosome-independent mitotic spindle formation in vertebrates. *Curr. Biol.* 10:59–67.

Kulp, D., D. Hausseler, M.G. Reese, and F.H. Eekman. 1996. A generalized hidden Markov model for the recognition of human genes in DNA. *Proc. Int. Conf. Intell. Syst. Mol. Biol.* 4:134–142.

Lukashin, A.V., and M. Borodovsky. 1998. Gene Mark.hmm: new solutions for gene finding. *Nucleic Acids Res.* 26:1107–1115.

Lupas, A., M. Van Dyke, and J. Stock. 1991. Predicting coiled coils from protein sequences. *Science.* 252:1162–1164.

Maniotis, A., and M. Schliwa. 1991. Microsurgical removal of centrosomes blocks cell reproduction and centriole generation in BSC-1 cells. *Cell.* 67:495–504.

Matsuura, K., P.A. Lefebvre, R. Kamiya, and M. Hirono. 2002. Kinesin-II is not essential for mitosis and cell growth in *Chlamydomonas. Cell Motil. Cytoskeleton.* 52:195–201.

Olmsted, J.B. 1981. Affinity purification of antibodies from diazotized paper bots of heterogeneous protein samples. *J. Biol. Chem.* 256:11955–11957.

Preble, A.M., T.H. Giddings Jr., and S.K. Dutcher. 2001. Extragenic bypass suppressors of mutations in the essential gene *BLD2* promote assembly of basal bodies with abnormal microtubules in *Chlamydomonas reinhardtii. Genetics.* 157:163–181.

Rieder, C.L., S. Faruki, and A. Khodjakov. 2001. The centrosome in vertebrates: more than a microtubule-organizing center. *Trends Cell Biol.* 11:413–419.

Ruiz, F., J. Beisson, J. Rossier, and P. Dupuis-Williams. 1999. Basal body duplication in *Paramecium* requires γ-tubulin. *Curr. Biol.* 9:43–46.

Ruiz, F., A. Krzywicka, C. Klotz, A. Keller, J. Cohen, F. Koll, G. Balavonie, and J. Beisson. 2000. The SM19 gene, required for duplication of basal bodies in *Paramecium*, encodes a novel tubulin, η-tubulin. *Curr. Biol.* 10:1451–1454.

Sager, R., and S. Granick. 1953. Nutritional studies with *Chlamydomonas reinhardtii. Ann. NY Acad. Sci.* 56:831–838.

Sambrook, J., E.F. Fritsch, and T. Maniatis. 1989. Extraction of RNA with guanidinium thiocyanate followed by centrifugation in cesium chloride solutions. *In* Molecular Cloning: A Laboratory Manual. Second edition. Cold Spring Harbor Laboratory Press, Cold Spring Harbor, NY. 7.19–7.22.

Shimogawara, K., S. Fujiwara, A. Grossman, and H. Usuda. 1998. High-efficiency transformation of *Chlamydomonas reinhardtii* by electroporation. *Genetics.* 148:1821–1828.

Silflow, C.D., M. La Voie, L.-W. Tam, S. Tousey, M. Sanders, W.-C. Wu, M. Borodovsky, and P.A. Lefebvre. 2001. The Vfl1 protein in *Chlamydomonas* localizes in a rotationally asymmetric pattern at the distal ends of the basal bodies. *J. Cell Biol.* 153:63–74.

Smith, E.F., and P.A. Lefebvre. 1996. *PF16* encodes a protein with armadillo repeats and localizes to a single microtubule of the central apparatus in *Chlamydomonas* flagella. *J. Cell Biol.* 132:359–370.

Stubblefield, E., and B.R. Brinkley. 1967. Architecture and function of the mammalian centriole. *In* Formation and Fate of Cell Organelles. K.B. Warren, editor. Academic Press, Inc., New York. 175–218.

Taillon, B.E., S.A. Adler, J.P. Suhan, and J.W. Jarvik. 1992. Mutational analysis of centrin: An EF-hand protein associated with three distinct contractile fibers in the basal body apparatus of *Chlamydomonas. J. Cell Biol.* 119:1613–1624.

Tam, L.-W., and P.A. Lefebvre. 1993. Cloning of flagellar genes in *Chlamydomonas reinhardtii* by DNA insertional mutagenesis. *Genetics.* 135:375–384.

Tamm, S., and S.L. Tamm. 1980. Origin and development of free kinetosomes in the flagellates *Deltotrichonympha* and *Koruga. J. Cell Sci.* 42:189–205.

Wright, R.L., B. Chojnacki, and J.W. Jarvik. 1983. Abnormal basal-body number, location, and orientation in a striated fiber-defective mutant of *Chlamydomonas reinhardtii. J. Cell Biol.* 96:1697–1707.

Wright, R.L., J. Salisbury, and J.W. Jarvik. 1985. A nucleus-basal body connector in *Chlamydomonas reinhardtii* that may function in basal body localization or segregation. *J. Cell Biol.* 101:1903–1912.